

May 2018

A Diagnostic Metric for Predicting Tropical Cyclone and Mid-Latitude Floods

Jonathon Klepatzki

Embry-Riddle Aeronautical University, klepatzj@my.erau.edu

Shawn M. Milrad

Embry-Riddle Aeronautical University, milrads@erau.edu

Follow this and additional works at: <https://commons.erau.edu/beyond>



Part of the [Atmospheric Sciences Commons](#), [Climate Commons](#), and the [Meteorology Commons](#)

Recommended Citation

Klepatzki, Jonathon and Milrad, Shawn M. (2018) "A Diagnostic Metric for Predicting Tropical Cyclone and Mid-Latitude Floods," *Beyond: Undergraduate Research Journal*: Vol. 2 , Article 2.

Available at: <https://commons.erau.edu/beyond/vol2/iss1/2>

This Article is brought to you for free and open access by the Journals at Scholarly Commons. It has been accepted for inclusion in Beyond: Undergraduate Research Journal by an authorized administrator of Scholarly Commons. For more information, please contact commons@erau.edu.

A Diagnostic Metric for Predicting Tropical Cyclone and Mid-Latitude Floods

Jonathon Klepatzki and Shawn M. Milrad

Abstract

This study details a dynamic and thermodynamic metric (i.e., Extreme Flood Index [EFI]) designed to diagnose the frequency and intensity of extreme precipitation events associated with stagnant mid-latitude flow patterns (i.e., Rex blocks). As the global climate warms, rapid Arctic warming may be helping to slow the mid-latitude westerly jet stream, resulting in increased mid-latitude flow stagnation. The combination of long-duration ascent associated with easterly winds and warm moist air increases the severity of extreme precipitation events; as such, the EFI is specifically designed to detect this potent combination of ingredients. In 2013, a Rex block stalled a low-pressure system over Alberta which caused the worst Canadian flood disaster ever seen. To that end, the recent billion-dollar flood catastrophe produced by Tropical Cyclone (TC) Harvey was also associated with a Rex Block (dynamics) in the presence of warm, moist air (thermodynamics). Despite dynamic differences between TC-related and mid-latitude floods, the EFI is successfully able to detect both. The dynamics component of the EFI is derived from two atmospheric blocking criteria, used operationally by the European Centre for Medium-Range Weather Forecasts (ECMWF) and National Oceanic and Atmospheric Administration (NOAA), respectively, and adapted here for the shorter duration of extreme precipitation events. The EFI's thermodynamic component utilizes standardized anomalies of equivalent potential temperature. Finally, the ability of the EFI to diagnose and predict high-impact flood events using reanalysis data and operational numerical weather prediction models is explored.

1. Introduction

In recent years, North America has experienced several high-impact billion-dollar extreme precipitation events associated with atmospheric flow stagnation. This research develops a metric to better diagnose and predict extreme floods associated with flow stagnation. Flow stagnation (i.e., a Rex block) occurs when an upper-tropospheric high-pressure system is located poleward of a low-pressure system and can help provide vast amounts of warm moist air conducive to extreme precipitation. An example of an extreme precipitation event can be seen in Fig. 1, in which tremendous amounts of precipitation accumulated over five days in August 2017, while TC Harvey was quasi-stationary over Texas. A textbook example of a Rex block (Rex 1950) is seen in Fig. 2, in which an upper-level high pressure (i.e., ridge) is located to the north of an upper-level low pressure (i.e., trough) over Texas. To distinguish these areas, the researchers analyzed synoptic patterns over the United States for anything that takes the shape of a hill (i.e., ridge) or a U (i.e., trough).

Earlier work on this project found that the most prominent and consistent mid-latitude EFI hotspots in the study period are found over the U.S. Rockies, as well as parts of Western Europe and the Mediterranean Sea (not shown). Dynamically, the transition seasons are dominated by the Polar Front Jet (PFJ) that becomes

more meridional (i.e., North to South movement) during this period, which increases the frequency of flow stagnation. However, flow stagnation is generally less frequent in both winter and summer.

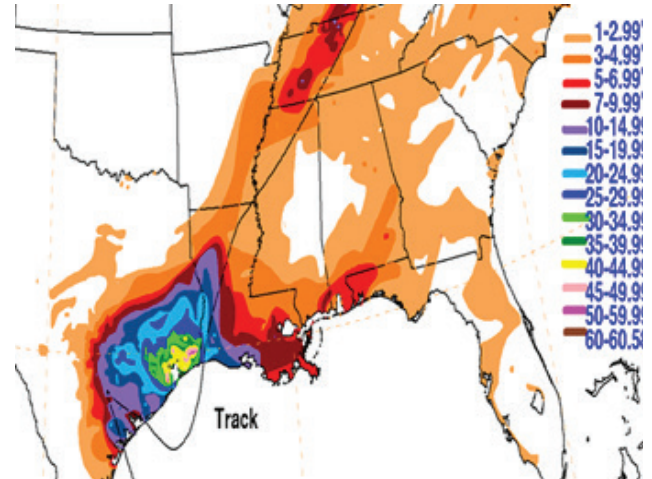


Figure 1: 25–31 August 2017 total precipitation (in., shaded) during the landfall of TC Harvey (NWS WPC 2018).

2. Methods

The EFI incorporates environmental ingredients that facilitate large precipitation rates for relatively long durations. The EFI is a multi-variate (thermodynamics + dynamics) metric,

$$EFI = B * \sigma_{\theta_e} * \frac{d}{dp}(r_s) * 1000 \quad (1)$$

where the value of the flow stagnation metric (B) is multiplied by the standardized anomaly of 700–400 hPa layer-averaged equivalent potential temperature (θ_e), the latter of which represents heat and moisture. The flow stagnation metric (B) is based on the aforementioned two operational blocking indices: a 500-hPa metric developed by Tibaldi and Molteni (1990) and used by the National Oceanic and Atmospheric Administration (NOAA), as well as the Dynamic Tropopause (DT) potential temperature (θ) metric of Pelly and Hoskins (2003a,b) that is used by the European Centre for Medium-Range Weather Forecasts (ECMWF). Both the 500-hPa and DT flow stagnation metrics were modified in time and space to account for the shorter duration of extreme precipitation events. This shorter duration was defined as a minimum 24-h period, compared to the five days specified by Tibaldi and Molteni (1990) and Pelly and Hoskins (2003a,b). The justification for the modified time requirement is that the original blocking indices were developed for longer-duration phenomena such as heatwaves and droughts, whereas extreme precipitation events generally occur on shorter timescales.

Calculations of each flow stagnation metric were performed as follows. For the 500-hPa metric:

- A reversal in the 500-hPa flow in the midlatitudes was identified when the zonal component of the geostrophic wind was $\leq -2.5 \text{ m s}^{-1}$. This threshold was predicated on a visual identification of a gradient reversal for a 500-hPa geopotential height contour interval of 30 m. At 45° N , a gradient of 30 m per 10° of latitude corresponds to an easterly geostrophic wind of approximately 5 kt (2.5 m s^{-1}). The use of a geostrophic wind threshold allowed for the metric to be calculated simultaneously for both the Northern and Southern Hemispheres.
- In the tropics (equatorward of 20°), very small pressure gradients can result in relatively large geostrophic winds. However, instead of limiting our metric by an arbitrary latitude, the researchers screened for values of DT pressure values of $< 150 \text{ hPa}$. Excluding these values removed the climatological trade winds.
- Once the above two criteria were met, a third criterion stipulated that the first two criteria had to be present at a grid point for a minimum duration of 24 h. For any grid point where all three criteria were met, a 500-hPa height flow stagnation metric = true was

recorded as “1” for the grid point. A 500-hPa height flow stagnation metric = false was recorded as a “0”. The researchers note that a “1” at any given time step means that the following 24 hours met the criteria; i.e., a “1” at 00 UTC 16 April indicates flow stagnation through 00 UTC 17 April. In addition, a “1” at a given grid point for two consecutive time periods should be interpreted as the presence of flow stagnation for 30 h, inclusive.

For the DT metric:

- DT pressure was utilized instead of potential temperature on the DT. This was done largely to avoid the relatively “noisy” structures of DT potential temperature associated with tropical bursts of convection, which would have obfuscated the results. While this was likely not an issue with the larger space and time scales of Pelly and Hoskins (2003a,b), the smaller time and space scales of our flow stagnation metric necessitated it. Physically, a strong upper-tropospheric trough is associated with a depressed tropopause and consequently a large value of pressure on the DT. Consequently, an equatorward-oriented pressure gradient would be indicative of smaller DT pressure values located equatorward of larger DT pressure values and would represent a reversal in the flow. A reversal in the DT pressure field was identified when the equatorward component of the gradient in pressure on the DT was $\geq 50 \text{ hPa per } 10^\circ$ of latitude normalized to 45° N . This is approximately equivalent to a gradient of 0.0045 Pa m^{-1} at 45° N . The normalization to this latitude was attained by multiplying the local gradient by the quotient of the Coriolis parameter at 45° N with the Coriolis parameter at the latitude of each grid point, while maintaining the 0.0045 Pa m^{-1} threshold. Consequently, the threshold is diminished (increased) for locations equatorward (poleward) of 45° N .

- This threshold was sufficient in practice to remove features associated with the trade winds and consequently there was no screening of the results by latitude or DT pressure as there was in the 500-hPa geopotential height flow stagnation metric.

- The same 24-h criterion was applied as in the 500-hPa geopotential height flow stagnation metric.

The spatial scale requirement of 10° of latitude was reduced from 20° in the original blocking metrics (Tibaldi and Molteni 1990; Pelly and Hoskins 2003a,b). However, once a list of TC and non-TC cases was developed, the researchers further modified the spatial scale such that it would use our default criterion for

non-TC cases and a higher resolution for TC cases. The researchers did this because TCs tend to be smaller systems and our relatively coarse default setting was having difficulty detecting flow stagnation associated with TCs. After substantial testing, the researchers determined that the higher-resolution EFI was able to detect mid-latitude floods in addition to TC-related events, with no degradation in accuracy. Thus, throughout this paper the researchers show only high-resolution EFI results, and the various settings for B are outlined in Table 1. Finally, using standardized θ_e , allows the EFI to function independently of season, and the layer-averaged vertical change in saturation mixing ratio (r_s) was included to eliminate spurious EFI maxima in polar regions.

For the EFI to be considered a success, historical flow stagnation climatologies and trends from 1979–2016 had to be evaluated over three (i.e. North America, Europe, Asia) regions. This evaluation also included correlations with El Niño Southern Oscillation (ENSO) values to determine if flow stagnation was more prevalent during a particular ENSO phase. The dataset used for the majority of the work was the ERA-Interim Reanalysis (Dee et al. 2011). To test whether the EFI was able to successfully diagnose and predict the extreme rainfall from both case studies in this paper (TC Harvey and the 2013 Alberta Flood), the researchers also used forecasts from the NOAA Global Forecast System (GFS) model.

Flow Stagnation Criterion (B)	Minimum Duration	Original Latitudinal Spatial Scale	High-Resolution Latitudinal Spatial Scale
500-hPa	24 h	10°	1.5°
DT	24 h	10°	1.5°

Table 1: Characteristics of each flow stagnation criterion (B in Eq. 1) used to calculate the EFI.

3. Results

3.1 TC Harvey

The EFI successfully predicted large areas of warm moist air over Texas (Figs. 2, 3) at the times of the flow stagnation for the 60, 72, and 84-h forecast from the 0000 UTC 25 August GFS model run (Fig. 2). The ERA-Interim and GFS EFI results correspond to the area of heaviest precipitation seen in Fig. 1. Thus, the researchers have confidence that the EFI can diagnose

and predict extreme rainfall associated with flow stagnation. It is also of note that the synoptic-scale patterns (i.e., 500-hPa geopotential height, Figs. 2, 3) were similar between the GFS and ERA-Interim. This gives the researchers additional confidence that the EFI can be used in predictive mode for extreme precipitation events associated with flow stagnation.

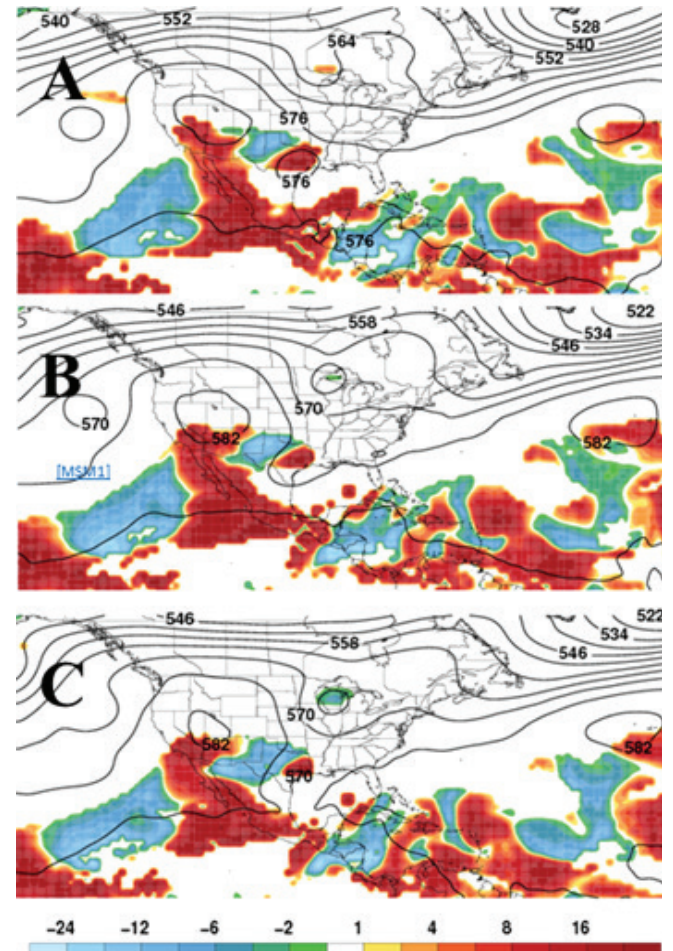


Figure 2: ERA-Interim high-resolution EFI (shaded) and 500-hPa geopotential height (decameters, solid black contours) for (a) 1200 UTC 27 August, (b) 0000 UTC 28 August, and (c) 1200 UTC 28 August. The EFI distinguished extreme rainfall over the Houston, Texas area produced by TC Harvey on 27–28 August 2017. Red indicates warm moist air (positive EFI values) while blue indicates dry air (negative EFI values).

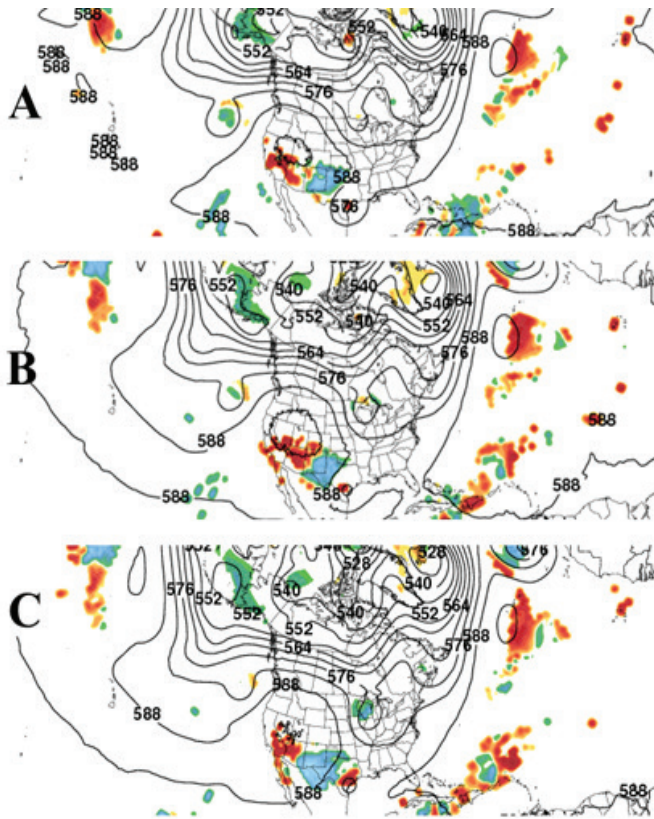


Figure 3: NOAA GFS model run at 0000 UTC 25 August 2017 showing high-resolution EFI (shaded) and 500-hPa geopotential height for forecasts at (a) 60 h (b) 72 h, and (c) 84 h, corresponding to the ERA-Interim panels in Fig. 2.

3.2 Alberta Flood

In 2013, Alberta was highly affected by a Rex block that forced strong easterly winds to ascend the eastern slopes of the Rocky Mountains, creating several days of moderate to heavy rain. This rainfall helped to create the largest flood disaster in Canadian history, with more than \$5 Billion USD in damage (Milrad et al. 2015). The flood was caused by a combination of meteorological, hydrological, and orographic processes (increased snowmelt, above-normal soil moisture, etc., Milrad et al. 2015). Orographic precipitation processes are related to the flow of wind ascending terrain such as the Rocky Mountains. The Alberta Flood occurred from 19-21 June 2013 in the foothills of the Rockies (average elevation 1200 m) and resulted in a total precipitation accumulation of 7–10 inches (Fig. 4).

By using the same analysis techniques as during the case study of TC Harvey, the EFI in both the GFS and the ERA-Interim demonstrated the ability to predict an extreme rainfall event associated with flow stagnation for the Alberta Flood. The regions of large EFI in Figs. 5 and 6 agree with the areas of heaviest precipitation seen

in Fig. 4.

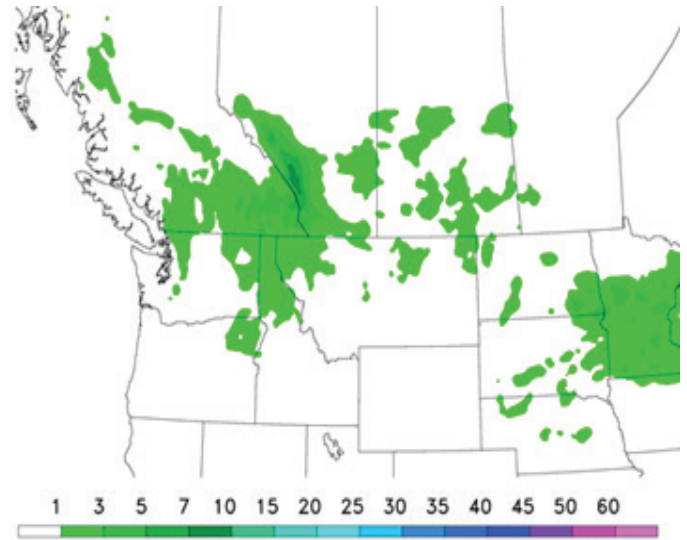


Figure 4: 72-h (19–21 June) total precipitation (in., shaded) during the 2013 Alberta, Canada Flood, from the Environment and Climate Change Canada Canadian Precipitation Analysis (CaPA, Mahfouf et al. 2007).

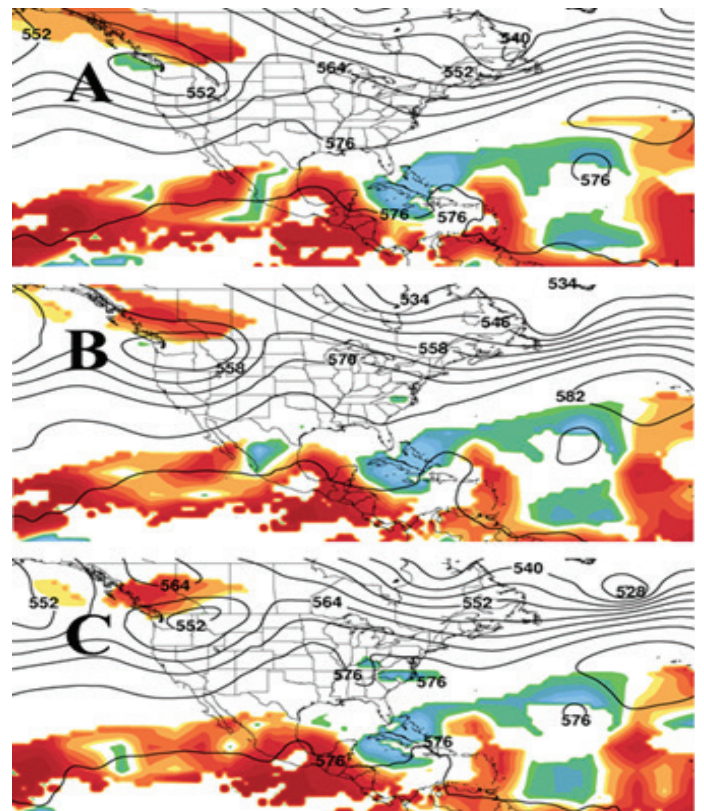


Figure 5: As in Fig. 2, but for the 2013 Alberta Flood at (a) 0000 UTC 20 Jun 2013 (b) 1200 UTC 20 Jun 2013, and (c) 0000 UTC 21 Jun 2013.

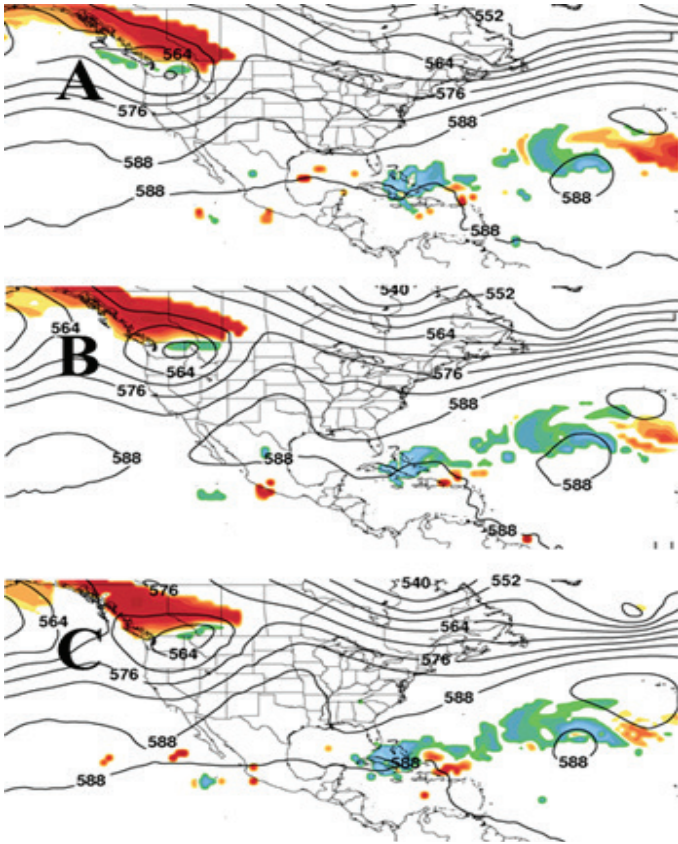


Figure 6: As in Fig. 3, but for the GFS model run at 0000 UTC 18 June 2013 for forecasts at (a) 48 h (b) 60 h, and (c) 84 h, corresponding to the ERA-Interim panels in Fig. 5.

4. Discussion

The EFI ERA-Interim analysis and the GFS forecasts demonstrate that the EFI is skillful in identifying floods associated with flow stagnation. It was found that flow stagnation, and thus large EFI events, are more prevalent on the lee side of large mountain ranges (e.g., Rockies, Alps), as the blocking large-scale flow patterns combined with orographic ascent of warm-moist air contribute significantly to the formation of rainfall. Future work includes evaluating the utility of the EFI with regards to systematic predictability of extreme flood events, including the determination of the EFI forecast skill within both deterministic and ensemble numerical weather prediction systems. Finally, an EFI forecast user interface will be created, through which enhancements to the prediction of extreme flood events will potentially save lives.

References

- Mahfouf, J. F., B. Brasnett and S. Gagnon, 2007: A Canadian precipitation analysis (CaPA) project: Description and preliminary results. *Atmos. Ocean*, **45**, 1–17.
- Milrad, S., J. R. Gyakum, and E. H. Atallah, 2015: A Meteorological Analysis of the 2013 Alberta Flood: Antecedent Large-Scale Flow Pattern and Synoptic-Dynamic Characteristics. *143*, 2817-2841.
- National Weather Service Weather Prediction Center (NWS WPC), 2018: Tropical cyclone rainfall data. Available online at <http://www.wpc.ncep.noaa.gov/tropical/rain/tcrainfall.html>.
- Pelly, J. L. and B. J. Hoskins, 2003: A new perspective on blocking. *J. Atmos. Sci.*, **60**, 743-760.
- Rex, D. F., 1950: Blocking action in the middle troposphere and its effect upon regional climate. Part I: An aerological study of blocking action. *Tellus*, **2**, 196–211.
- Tibaldi, S., and F. Molteni, 1990: On the operational predictability of blocking. *Tellus*, **42A**, 343-365.